Mechanisms of reduction of MoO3 to MoO2 reconciled?

ARTICLE · JANUARY 2001

Source: OAI

4 AUTHORS:

E. Lalik
Jerzy Haber Institute of Catalysis and Surfac…
41 PUBLICATIONS **406** CITATIONS
SEE PROFILE

Bill David
Science and Technology Facilities Council
315 PUBLICATIONS **9,396** CITATIONS
SEE PROFILE

Paul Barnes
University College London
161 PUBLICATIONS **2,681** CITATIONS
SEE PROFILE

John Turner
University of Sussex
55 PUBLICATIONS **810** CITATIONS
SEE PROFILE

Mechanisms of Reduction of MoO_3 to MoO_2 Reconciled?

Erwin Lalik,[†,‡,||] William I. F. David,[‡] Paul Barnes,*[,†] and John F. C. Turner[§]

Industrial Materials Group, Department of Crystallography, Birkbeck College, Malet St., London WC1E 7HX, The ISIS Facility, Rutherford Appleton Laboratory, Chilton, Didcot, Oxon OX11 0QX, and The Royal Institution of Great Britain, 21 Albermarle St., London W1X 4BS

Received: April 27, 2001

The topotactic mechanism for the reduction of MoO_3 to MoO_2 has been well-supported by experiments, though the detection of Mo_4O_{11} during the process has been a challenge to the notion of direct conversion. In this study, high quality in-situ Neutron Powder Diffraction (NPD) has been used to monitor phase composition during the reduction of MoO_3 in a flow of hydrogen at 550 °C. Three phases have been detected: MoO_3, MoO_2, and Mo_4O_{11}. Multiphase Rietveld refinement has been used to obtain concentration profiles for all three oxides throughout the reduction process. Examination of these profiles reveals the following: (1) a higher content, initially, of MoO_2 than Mo_4O_{11}; (2) a period of constant MoO_2 content; (3) an induction period of Mo_4O_{11} formation; and (4) a resumption in growth of MoO_2 but with different unit cell dimensions.

1. Introduction

Reducibility of MoO_3 is conducive to its most important applications: in heterogeneous catalysis the ability of MoO_3 to release lattice oxygen is instrumental in the selective oxidation of hydrocarbons; in metallurgy, the reduction of α-MoO_3 to MoO_2 is the first, crucial, stage in the extraction of metallic molybdenum.[1] Reduction is typically performed at 600 °C using gaseous hydrogen as the reducing agent and chemical grade tungsten-free molybdena as the starting material.

The first mechanism proposed was the direct reduction model

$$MoO_3 + H_2 = MoO_2 + H_2O \quad (1)$$

with the diffusion of oxygen vacancies from the surface believed to be the rate-determining step.[2] Later, a detailed structural mechanism for a topotactic MoO_3/MoO_2 transition was proposed.[3] However, examination of the reaction mixture during reduction revealed that in some cases the so-called mixed-valence oxides, mainly the orthorhombic Mo_4O_{11}, have also been found.[4−6] This prompted the idea that Mo_4O_{11}, which is structurally related to metastable (perovskite-type) β-MoO_3,[7,8] might be an intermediate between MoO_3 and MoO_2, leading to an alternative "consecutive" model of reduction

$$4MoO_3 + H_2 = Mo_4O_{11} + H_2O \quad (2a)$$

$$Mo_4O_{11} + 3H_2 = 4MoO_2 + 3H_2O \quad (2b)$$

Whether or not Mo_4O_{11} appears seems to depend on the reaction conditions or preparation of the starting material.[6] The literature shows that the direct mechanism is well supported by experiments, though it can be argued that the frequent absence of Mo_4O_{11} is simply a failure of detection. Conventional in-situ X-ray diffraction can realize only limited time resolution and sample penetration: e.g., a Cu−Kα X-ray source penetrates the top 10−20 μm of an α-MoO_3 sample which itself displays pronounced preferred orientation. By comparison, relatively short collection times can be achieved with an intense neutron source and samples can be large enough to avoid the problems of preferred orientation. Furthermore, the neutron scattering cross sections for oxygen and molybdenum, being rather similar (4.23×10^{-28} and 6.09×10^{-28} m^2 respectively), lead to sensitivity in measurement of the oxygen content and accurate positioning of Mo/O sites for each reactant, unlike the X-ray case where molybdenum scatters far more strongly than oxygen.

In this study, we present high quality time-resolved in-situ NPD results on the reduction of α-MoO_3 to MoO_2, using multiphase Rietveld refinement to quantitatively determine the concentrations of the reactants throughout the 123 patterns taken during the 20 h experiment.

2. Experimental and Analysis Methods

Materials and Procedure. The material used was commercial α-MoO_3 (BDH AnalaR, 99.5%), recrystallized at 600 °C for 24 h in a flow of oxygen to ensure a standard well-crystallized sample without β-MoO_3 impurities. The flow reactor for the in-situ NPD was 10 mm in diameter and made of gold-lined vanadium/titanium alloy; the amount of sample used was ∼10 g and the height of the bed inside the reactor was 50 mm. The temperature was measured by two thermocouples placed at the top and bottom of the reactor. The reduction was carried out at 550 °C in a gas mixture containing 30% hydrogen and 70% helium flowing at a rate of 30 cm^3/min. The reactor was placed within the pathway of the neutron beam, and time-of-flight NPD measurements were carried out in-situ on the POLARIS diffractometer at the ISIS Facility of Rutherford Appleton Laboratory. The acquisition time for each diffraction pattern was 10 min.

Data Analysis. Each diffractogram has been subjected to multiphase Rietveld refinement using only the data from the

* To whom correspondence should be addressed. barnes@img.cryst.bbk.ac.uk

† Industrial Materials Group, Department of Crystallography, Birkbeck College.

‡ The ISIS Facility, Rutherford Appleton Laboratory.

§ The Royal Institution of Great Britain.

|| On leave from Institute of Catalysis and Surface Science of Polish Academy of Science, ul. Niezapominajek, 30−239 Krakow, Poland.

10.1021/jp011622p CCC: $20.00
Published on Web 08/25/2001

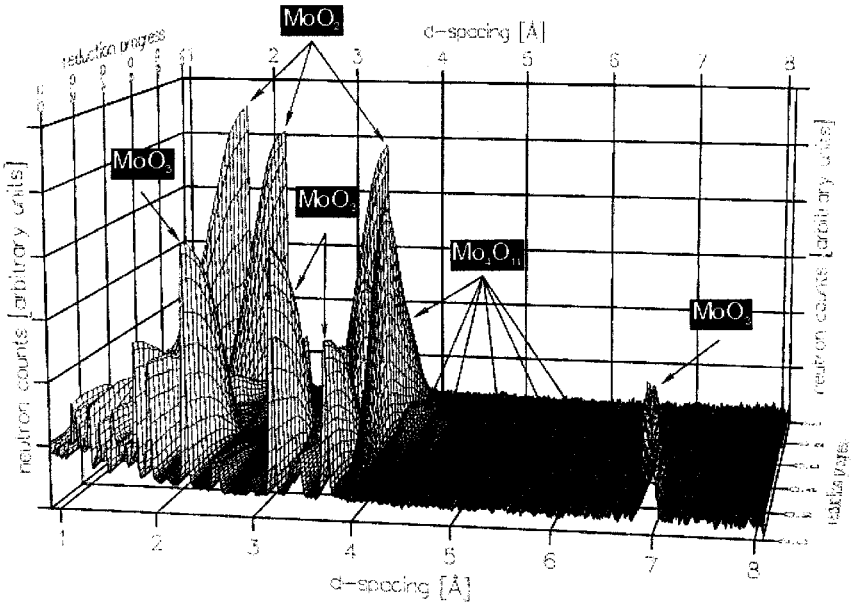

Figure 1. 3-dimensional overview of the whole neutron powder diffraction experiment showing the various changes in intensity of Bragg peaks during the progressive reduction of MoO_3 in hydrogen at 550 °C.

35° detector bank which covers a *d* spacing range of 0.905−8.083 Å (time-of-flight 2000−17 867 μs): the reason for this restriction was that in practice only the 35° detector bank provides a sufficient number of diffraction peaks from each of MoO_3, Mo_4O_{11}, and MoO_2, particularly in the case of long *d* spacing reflections from MoO_3 and Mo_4O_{11}, for a quantitative multiphase refinement giving similar importance to the (three) principal phases. The Rietveld refinement code was written at ISIS (based on the Cambridge Crystallography Subroutine Library (CCSL)) using the Voigt function convoluted with a double-exponential function to describe the peak shape.[9] Good fits have been achieved for all except two patterns (consequently rejected), the chi-squared values being usually less than 1.2. Examples of these multiRietveld plots are shown in Figure 2.

Calculation of Phase Content. Multiphase refinement yields fractional scale factors, S_i, for each individual phase i. These are related to the corresponding mass, m_i, of the phase by the following formula:

$$m_i = S_i Z_i M_i V_i C \tag{3}$$

where Z_i is the number of formula units per unit cell, M_i is the molecular mass, V_i is the unit cell volume and C is a constant.[10] Dividing by M_i yields

$$n_i = S_i Z_i V_i C \tag{4}$$

where n_i is the number of moles of each phase. The molar fraction for each phase, x_i, can then be calculated as

$$x_i = \frac{S_i Z_i V_i}{\sum_i S_i Z_i V_i} \tag{5}$$

The resulting molar fractions for each phase during reduction are shown in Figure 3 using $Z_i = 4$, 16, 4, respectively for the MoO_3, $MoO_{2.75}$ and MoO_2 formula units.

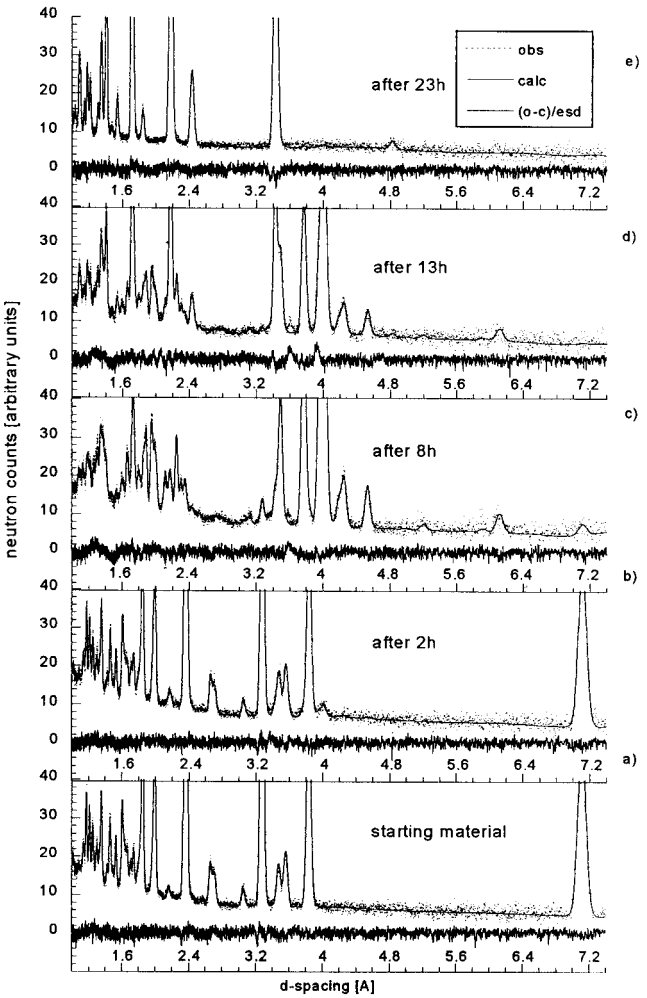

Figure 2. Neutron powder diffraction patterns and their multiphase (MoO_3, Mo_4O_{11}, MoO_2) Rietveld refinement plots of the reaction mixture at characteristic points during the reduction of MoO_3.

3. Results

Phase Composition. The three principal phases detected (Figure 1) are MoO_3, MoO_2, and orthorhombic γ-Mo_4O_{11} in addition to traces of monoclinic η-Mo_4O_{11}. The η-Mo_4O_{11} is revealed by the small reflection at ca. 3.6 Å (just perceptible in Figure 2c,d) which is in fact the most intense reflection in the

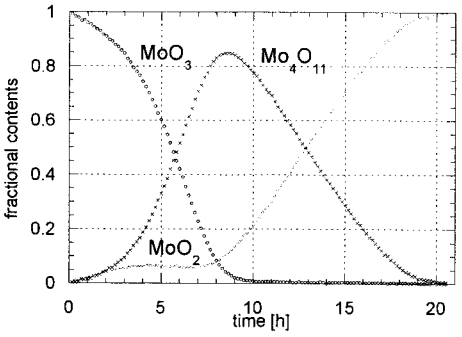

Figure 3. Phase concentration vs time profiles (from data in Figure 1), normalized to relative moles of MoO_3, MoO_2, and Mo_4O_{11}, obtained from time-resolved multiphase Rietveld analysis.

neutron diffraction pattern for η-Mo_4O_{11}. This represents a negligible level in quantitative terms and is therefore not included in the multiphase Rietveld refinement, though it is indeed notable that η-Mo_4O_{11} has now been detected during the reduction of MoO_3 for the first time even if such trace amounts means that it cannot play a significant role in the overall reaction mechanism. Visual inspection (Figures. 1, 3) shows that the buildup of Mo_4O_{11} is initially slow, reminiscent of an induction period, with a maximum around 8 h. The MoO_2 content over this same 8 h period is small but grows rapidly after 8 h.

Reaction Sequence. The reduction sequence can be divided into three stages:

1. (0−3 h) An induction-like period of Mo_4O_{11} formation in which the concentration of MoO_2 is higher than that of Mo_4O_{11};

2. (3−8 h) A rapid depletion of MoO_3 accompanied by a rapid increase of Mo_4O_{11} content reaching a maximum after ca. 8 h;

3. (8−20 h) The MoO_3 becomes fully depleted, the Mo_4O_{11} decreases and is fully consumed, whereas the MoO_2 content increases again reaching completion.

Variation in Lattice Constants. Full Rietveld refinements are first conducted to give the best set of atom (fractional) coordinates at the times when the three principal phases are respectively at their maxima (i.e., MoO_3 at time zero, Mo_4O_{11} at 8 h and MoO_2 at 20 h). For quantitative multiphase refinement, it is common practice to allow the unit cell parameters of each phase to vary with the weight fractions during refinement (to accommodate small peak shifts) using the best (fixed) set of fractional coordinates for each phase. Consequently, a clear change in lattice parameter can be significant even though the changes in *relative* intensity within each phase are too small for meaningful structural interpretation. Figure 4 shows the time variations in the lattice constants for the product MoO_2 obtained in this way. The **a** and **c** constants appear to change significantly on entering the third stage, whereas the **b** constant remains static. One might consider that this change corresponds to the differing porosity/defect characteristics of the MoO_2 structure formed from two different precursors (MoO_3 and Mo_4O_{11}) though such speculation is premature at this stage; the actual change however provides a clear hint of there being two types of MoO_2 formation, and this observation is also noted in section 4.

4. Discussion

The above results are discussed in relation to candidate mechanisms for the reduction of MoO_3 to MoO_2. Clearly, any successful description must account for the presence of the intermediate Mo_4O_{11} which has been widely studied over the last two decades as part of an extensive literature[2−7,11−32] surrounding the reduction of MoO_3. Four candidate mechanisms are given.

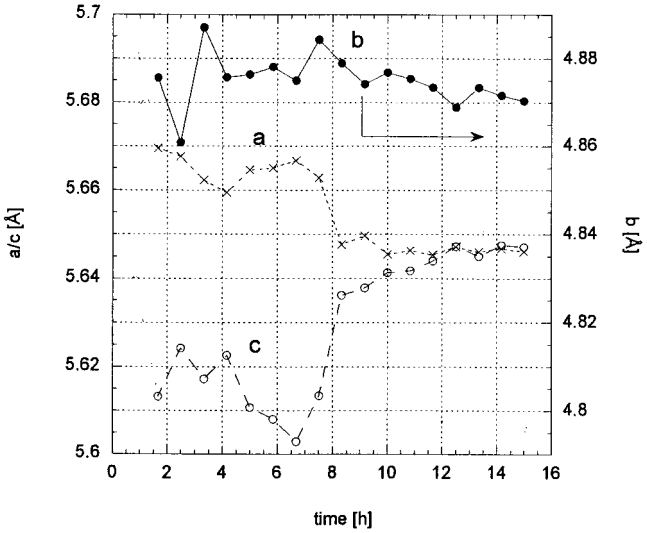

Figure 4. Variations obtained in lattice constants for MoO_2 during the reduction process, showing two clear time regimes (0−7; 8−16 h) for the **a**- and **c**-unit cell parameters.

Topotactic Mechanism. The majority of studies appear to favor a direct reduction of MoO_3 to MoO_2. The topotactic mechanism proposed for this transition[3] assumes slip between adjacent MoO_3 bi-layers which collapse together with removal of any water molecules or hydroxyl groups along the (010) layers. Reduction starts on the basal (010) plane of MoO_3 and proceeds toward the grain center, maintaining the crystal habit. Although the topotactic process has been well supported experimentally, it cannot reconcile the presence of an intermediate phase.

Consecutive Mechanism. This refers to the classic three-phase sequence, $MoO_3 \rightarrow Mo_4O_{11}$ (intermediate) $\rightarrow MoO_2$ (eqs 2a,b), the rates of each step depending on the form of MoO_3 and the reducing conditions.[4−6] In an extreme case (that of step 2b being much faster than 2a), the Mo_4O_{11} concentration would remain small throughout the process, which could partly account for the scarcity of Mo_4O_{11} encounters in the literature. Credence to this mechanism is gained from the simple mole-balance (Figure 3), which shows that most of the MoO_3 is converted to Mo_4O_{11} and then subsequently to MoO_2. However, this mechanism cannot on its own account for the plateau in MoO_2-formation.

Comproportionation. This mechanism can take into account our observation that MoO_2 initially rises faster, than Mo_4O_{11}, prior to the plateau at ∼3 h. Mo_4O_{11} is then formed by comproportionation of MoO_3 and MoO_2 according to

$$MoO_3 + H_2 = MoO_2 + H_2O \quad (6a)$$

$$3MoO_3 + MoO_2 = Mo_4O_{11} \quad (6b)$$

$$Mo_4O_{11} + 3H_2 = 4MoO_2 + 3H_2O \quad (6c)$$

This sequence can even accommodate topotactic aspects in stages 6a,b, but it is difficult to reconcile the sustained MoO_2 plateau unless one invokes a steady state balance between MoO_2 formation and consumption (6a,b) between 3 and 8 h.

Competitive Nucleation. This requires at least two parallel routes (7a; 7b + 7c) of MoO_2 formation through three component stages

$$MoO_3 + H_2 \rightarrow MoO_2 + H_2O \quad (7a)$$

$$4MoO_3 + H_2 \rightarrow Mo_4O_{11} + H_2O \quad (7b)$$

$$Mo_4O_{11} + 3H_2 \rightarrow 4MoO_2 + 3H_2O, \quad (7c)$$

each rate being highly sensitive to the number of product nuclei present. At first (0−2 h), there will be few nuclei present of either MoO_2 or Mo_4O_{11} and 7a and 7b will both proceed slowly; however, if 7b is highly sensitive to nucleation it will accelerate once sufficient Mo_4O_{11} nuclei have formed (>3 h) to dominate the sequence, starving 7a of its essential MoO_3. This kinetic combination can fully account for our observations, in particular the MoO_2 plateau and the two lattice constant time regimes (0−7; 8−20 h; Figure 4) which correspond to the two routes (7a, 7c) of MoO_2 formation. Similar reasoning has been used elsewhere for the hydration of calcium aluminate cements.[33,34]

5. Conclusions

The high quality data presented here unambiguously confirm the presence of the orthorhombic Mo_4O_{11} during reduction of MoO_3. The mole balance sheet, from the multiphase Rietveld refinement, demonstrates that Mo_4O_{11} plays an intermediate role for most of the reduction sequence, in agreement with previous reports.[4,5] The scarcity of Mo_4O_{11} sightings in the literature might be attributed to variations in material and conditions, combined with inferior time-resolutions; even the positive sightings to date[4,5] consisted of only 8 and 4 experimental points, whereas in this study, 123 in-situ patterns were collected during typical reduction.

Of the candidate models considered, the Topotactic and Consecutive mechanisms are both considered to be inadequate, on their own, in explaining the key features. The Comproportionation mechanism is capable of being reconciled with a Topotactic process (eq 6a) and can account for the MoO_2 plateau provided one accepts an exact balancing in MoO_2 formation/consumption during the first two stages. The Competitive Nucleation mechanism plausibly accounts for the observed MoO_2 plateau and the variation in lattice constants.

References and Notes

(1) Braithwaite, E. R. In Molybdenum: *An Outline of its Chemistry and Uses, Studies in Inorganic Chemistry*; Braithwaite, E. R., Haber, J., Eds.; Elsevier, Amsterdam, 1994; Vol. 19, Chapter 1, p 20.

(2) Kennedy, M. J.; Bevan, S. C. *J. Less Common Met.* **1974**, *36*, 23.

(3) Dufour, L. C.; Bertrand, O.; Floquet, N. *Surf. Sci.* **1984**, *147*, 396.

(4) Ueno, A.; Kotera, Y.; Okuda, S.; Bennet, C. O. *Proc 5th Int. Conf. Climax* **1982**, p 250.

(5) Sloczynski, J.; Bobinski, W. J. *Solid State Chem.* **1991**, *92*, 436.

(6) Burch, R. *J. Chem. Soc., Faraday Trans. 1* **1978**, *74*, 2982.

(7) Kihlborg, L. *Adv. Chem. Ser.* **1963**, *39*, 37.

(8) McCarron, E. M. III. *J. Chem. Soc., Chem. Commun.* **1986**, 336.

(9) David, W. I. F.; Jorgensen, J. D. In *The Rietveld Method*; Young, R. A., Ed.; Oxford University Press: 1996; pp 203, 205.

(10) Hill, R. J.; Howard, C. J. *J. Appl. Crystallogr.* **1987**, *20*, 467.

(11) Svensson, G.; Kihlborg, L. *Reactivity of Solids* **1987**, *3*, 33.

(12) Hansen, S.; Andersson, A. *Inst. Phys. Conf. Ser. No.93* **1998**, *2*, 279.

(13) von Destinon-Forstmann, J. *Can. Metall. Q.* **1965**, *4*, 1.

(14) Bursill, L. A.; Dowell, W. C. T.; Godman, P.; Tate, N. *Acta Crystallogr. A* **1977**, *34*, 296.

(15) Orehotsky, J.; Jamiolkowski, L.; Gerboc, J. *Mater. Sci. Eng.* **1979**, *41*, 237.

(16) Carpanter, K. H.; Hellada, C. J. In *Proceedings, Climax 3rd International Conference on the Chemistry and Uses of Molybdenum*; Barry, P. C., Mitchell, C. H., Eds.; Ann Arbour, 1979; p 204.

(17) Gai, P. L. *Philos. Mag. A* **1981**, *43*, 841.

(18) Gai, P. L.; Labun, P. A. *J. Catal.* **1985**, *94*, 79.

(19) Firment, L. E.; Faretti, A. *Surf. Sci.* **1983**, *129*, 155.

(20) Dominuez-Esquivel, J. M.; Fuentes-Moyado, S.; Diaz-Guerrero, G.; Vazquez-Zavala, A. *Surf. Sci.* **1986**, *175*, L701.

(21) Anderson, A.; Hansen, S. *J. Solid State Chem.* **1988**, *75*, 225.

(22) Spevack, P. A.; McIntyre, N. S. *J. Phys. Chem.* **1992**, *96*, 9029.

(23) Smith, R. L.; Rohrer, G. S. *J. Catal.* **1996**, *163*, 12.

(24) Kuzmin, A.; Purans, J.; Parent, Ph.; Dexpert, H. *J. Phys IV France* **1997**, *7*, C2−891.

(25) Haber, J.; Lalik, E. *Catal. Today* **1997**, *33*, 119.

(26) Ledain, S.; Leclaire, A.; Borel, M. M.; Provost, J.; Raveau, B. *J. Solid State Chem.* **1998**, *140*, 128.

(27) Roussel, P.; Labbé, Ph.; Groult, D.; Domengès, B.; Leligny, H.; Grebille, D. *J. Solid State Chem.* **1996**, *122*, 281.

(28) Domengès, B.; Roussel, P.; Labbé, Ph.; Groult, D. *J. Solid State Chem.* **1996**, *127*, 302.

(29) Bhuvanesh, N. S. P.; Gopalakrishnan, J. *J. Mater. Chem.* **1997**, *7*, 2297.

(30) Portemer, F.; Sundberg, M.; Kihlborg, L.; Figlarz, M. *J. Solid State Chem.* **1993**, *103*, 403.

(31) D′Yachenko, O. G.; Tabachenko, V. V.; Sundberg, M. *J. Solid State Chem.* **1995**, *119*, 8.

(32) Kahruman, C.; Yusufoglu, I.; Oktay, E. *Trans. 1nstn. Min. Metall. (Sect. C: Mineral Process. Extr. Metall.)* **1999**, *108*, C8.

(33) Rashid, S.; Barnes, P.; Bensted, J.; Turrillas, X. *J. Mater. Sci. Lett.* **1994**, *13*, 1232.

(34) Jupe, A. C.; Turrillas, X.; Barnes, P.; Colston, S. L.; Hall, C.; Häusermann, D.; Hanfland, M. *Phys. Rev. B.* **1996**, *53*, 14697.